EDITOR
F. RICHARD KEENE

Chirality in Supramolecular Assemblies

Causes and Consequences

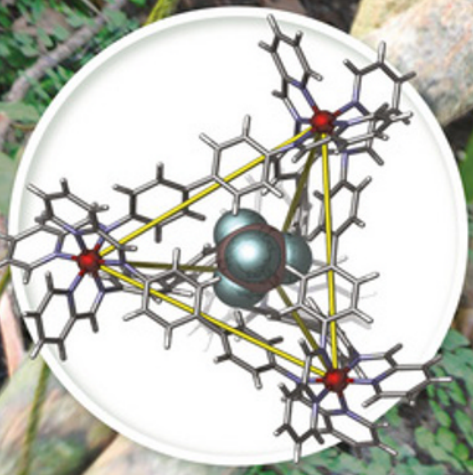

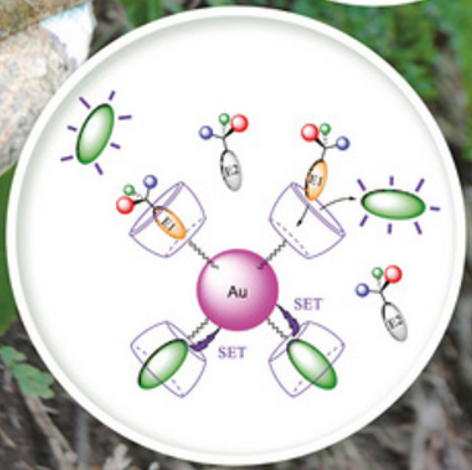

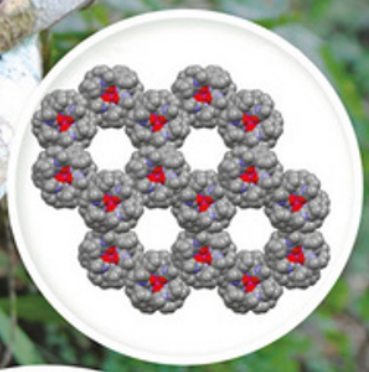

WILEY

Chirality in Supramolecular Assemblies

Chirality in Supramolecular Assemblies

Causes and Consequences

Edited by

F. RICHARD KEENE

Department of Chemistry,
School of Physical Sciences,
University of Adelaide, Australia

WILEY

This edition first published 2017

Registered Office
John Wiley & Sons, Ltd, The Atrium, Southern Gate, Chichester, West Sussex, PO19 8SQ, United Kingdom

Library of Congress Cataloging-in-Publication data applied for

A catalogue record for this book is available from the British Library.

ISBN: 9781118867341

Set in 10/12pt Times by SPi Global, Pondicherry, India

10 9 8 7 6 5 4 3 2 1

Contents

List of Contributors

David B. Amabilino, School of Chemistry, University of Nottingham, Nottingham, United Kingdom

Paul D. Beer, Inorganic Chemistry Laboratory, University of Oxford, Oxford, United Kingdom

Roger Bishop, School of Chemistry, The University of New South Wales, Sydney, Australia

Jean-Claude Chambron, Institut de Chimie Moléculaire de l'Université de Bourgogne, Dijon, France

Pedro Cintas, Departamento de Química Orgánica e Inorgánica, Facultad de Ciencias, Universidad de Extremadura, Badajoz, Spain

Jack K. Clegg, School of Chemistry and Molecular Biosciences, The University of Queensland, Brisbane, Australia

Steven De Feyter, Division of Molecular Imaging and Photonics, Department of Chemistry, KU Leuven-University of Leuven, Leuven, Belgium

Iris Destoop, Division of Molecular Imaging and Photonics, Department of Chemistry, KU Leuven-University of Leuven, Leuven, Belgium

Christopher J. Easton, Research School of Chemistry, Australian National University, Canberra, Australia

Nicholas H. Evans, Department of Chemistry, Lancaster University, Lancaster, United Kingdom

Daniel Fankhauser, Research School of Chemistry, Australian National University, Canberra, Australia

Philip A. Gale, Chemistry, University of Southampton, Southampton, United Kingdom

Declan P. Gavin, Department of Chemistry, Synthesis and Solid State Pharmaceutical Centre, University College Cork, Cork, Ireland

F. Richard Keene, Department of Chemistry, School of Physical Sciences, University of Adelaide, Adelaide, Australia

Jonathan A. Kitchen, Chemistry, University of Southampton, Southampton, United Kingdom

Edward G. Latter, Surface Science Research Centre and the Department of Chemistry, University of Liverpool, Liverpool, United Kingdom

Anita R. Maguire, School of Pharmacy and Department of Chemistry, Analytical and Biological Chemistry Research Facility, Synthesis and Solid State Pharmaceutical Centre, University College Cork, Cork, Ireland

John C. McMurtrie, School of Chemistry, Physics and Mechanical Engineering, Queensland University of Technology, Brisbane, Australia

Rasmita Raval, Surface Science Research Centre and the Department of Chemistry, University of Liverpool, Liverpool, United Kingdom

David R. Turner, School of Chemistry, Monash University, Clayton, Australia

Preface

The origins of what is now called *supramolecular chemistry* have been somewhat disparate, arising in part from studies of the chemistry of macrocycles (a development of naturally occurring analogues), spherands and carcerands, and cryptates . . . but the award of the 1987 Nobel Prize to Donald Cram, Charles Pedersen and Jean-Marie Lehn in many ways gave it a consolidated focus and led to its emergence as a field that retains vigorous and distinctly multidisciplinary activities. Supramolecular chemistry – defined by Lehn as "the chemistry of molecular assemblies and of the intermolecular bond" – deals with the organization of molecules into defined assemblies using noncovalent interactions, including weaker and reversible associations such as hydrogen bonds, π-π interactions, dispersion interactions, hydrophobic and solvophobic effects, and metal-ligand interactions. The aspect of stereochemistry within such chemical architectures, and in particular *chirality*, is of very special interest as it impacts on considerations of molecular recognition, the development of functional materials, the vexed question of homochirality, nanoscale effects of interactions at interfaces, biocatalysis and enzymatic catalysis, and applications in organic synthesis.

This book is intended to address the nature of the phenomenon of chirality in its broadest sense, noting the change in its nuances and subtlety in the progression from simple individual molecules to molecular assemblies, and to show the manifestations of chirality in the synthesis, properties, and applications of supramolecular systems, emphasizing their multidisciplinary importance.

The book is essentially divided in to four broad parts. The first constitutes an introduction to chirality: Chapter 1 develops the concept of chirality from rigid isolated molecules through to assemblies of molecules (in supramolecular entities), to topological chirality. Chapter 2 discusses chirogenesis and the phenomenon of homochirality (loss of parity) in the development of naturally occurring polymers (including nucleic acids and polypeptides) – and its consequences for the formation of artificial supramolecular

aggregates. Chapter 3 provides an overview of chiral aspects arising in the crystallization of small organic molecules – principles that are applicable to all classes of molecules, including supramolecular assemblies.

The second part is predominantly (but not exclusively) centered on metallosupramolecular chemistry. By the use of examples, Chapter 4 addresses the diversity of supramolecular assemblies – and in particular metallosupramolecular assemblies – and describes the complexity of chiral structures and their construction through self-assembly procedures. Chapter 5 describes the role of chirality in molecular recognition and host-guest systems. Chapter 6 develops the notion that unique characteristics can be built into supramolecular assemblies because of features of chirality – characteristics that can lead to functional properties of such materials. Chapter 7 addresses bulk homochiral solids formed using chiral reagents – either by direct incorporation, or by templating or induction, during synthesis. Chapter 8 considers the basic design principles that underpin the construction of metallosupramolecular polyhedra.

The third part is devoted to chirality at interfaces. Chapter 9 focuses on chirality expression and amplification at solution / solid-state interfaces, and applications such as heterogeneous catalysis and chiral separations. Chapter 10 addresses the initiation of chiral suprastructures on surfaces, and their modeling by high-resolution experimental methods and theoretical calculations.

The fourth part addresses chirality in organic hosts, and in biological / enzymatic systems: organic hosts are used in analytical chemistry to separate racemic guest mixtures or simply to distinguish enantiomers, and chiral hosts can function as catalysts in asymmetric reactions – Chapter 11 reviews particular features and applications of chiral organic host systems based primarily on cyclodextrins, calixarenes, and crown ethers in this regard. Chapter 12 stresses the enormous potential of microorganisms and enzymes as catalysts in asymmetric synthesis for controlling the stereochemical outcome of reactions, and discusses the use of whole cells and isolated enzymes as an attractive option for the chemical industry.

It is always understood that supramolecular chemistry is so diverse that one book cannot be totally equitable in its coverage of all aspects of the field. This book attempts to address some of the major aspects authoritatively and highlight important current thrusts. It will be useful to researchers working with chiral supramolecular assemblies, and will hopefully draw others with an existing interest in supramolecular systems to a further appreciation of the importance of chirality in the field, as seen through contributions of experts in their respective parts of that firmament.

F. Richard Keene
Adelaide, Australia

1

Principles of Molecular Chirality

Jean-Claude Chambron and F. Richard Keene

1.1 General Introduction

Chirality is probably one of the most significant topics in chemistry. The strong connection between chirality and symmetry has made it appealing from the mathematical and aesthetic viewpoints, and the recent interest in topologically chiral interlocked and knotted molecules has increased its intellectual attraction, raising the concept of a hierarchy in chirality [1]. The most fascinating aspect of chirality stems from the dynamic properties of molecules and supramolecular assemblies, rather than their static properties, because they are the cause of many intriguing and sometimes paradoxical issues. At the same time, dynamic chirality is also the most useful topic because of the numerous applications it underpins, from chiral recognition to molecular motors.

Historically, chirality is rooted into crystallography (the concept of hemiedry), and the first breakthrough into the field of molecular chirality was Louis Pasteur's hypothesis that the dissymmetry of a crystal was a consequence of dissymmetry at the molecular level [2]. The second milestone was the Le Bel and van't Hoff model of the tetrahedral carbon atom, which accounted for the chirality of the organic compounds known at that time, and several years later Werner was the first to study and provide evidence for the chirality of metal complexes. The discovery of organic molecules that did not owe their chirality to tetrahedral carbon atoms carrying four different substituents (e.g., allenes, biphenyls, cyclophanes), and of helical structures in nucleic acids and proteins, finally led Cahn, Ingold, and Prelog to establish a general system for the description of chiral structures. Since then, many novel chiral molecules have been reported, and most of them could be described in the frame of the CIP rules. The most notable developments in chirality in recent decades concern aspects of the generation and control of chirality: transfer by supramolecular

Chirality in Supramolecular Assemblies: Causes and Consequences, First Edition. Edited by F. Richard Keene.

interactions; chirality of molecular assemblies (chirality at the supramolecular level or "supramolecular chirality"); and finally, the concept of "topological chirality" brought forward by the development of interlocked and knotted molecules.

This chapter constitutes an introduction to molecular chirality from the rigid geometrical model to the topological model, but also from the isolated molecule to assemblies of molecules. As the first chapter in this book on the causes and consequences of chirality in supramolecular assemblies, it will, nevertheless, not cover all the aspects of chirality transfer – in particular those resulting from a covalent bond formation.

1.2 Geometrical Chirality

A chiral object is the one that does not coincide with its mirror image. The source object and its mirror image are called enantiomorphs. From the point of view of symmetry, enantiomorphic objects can have only rotation axes C_n, $n \geq 1$, as symmetry elements: they are either asymmetric (C_1) or dissymmetric (C_n, $n \neq 1$). There are many natural examples of enantiomorphic objects, the prototypical one being the human hand, the Greek word for which (χειρ) has been used to create the English word "chiral." Molecules are objects at the nanometer scale that are made of atoms connected by chemical bonds. If molecules are considered as rigid nanoscale objects, the definition given above can be very easily transposed to the molecular level, with the term "enantiomorph" being replaced by "enantiomer." However, molecules differ from macroscopic objects according to two criteria: (i) they are not rigid and can encompass a great variety of shapes called conformations, the distribution of which depends on time, temperature, and solvent; (ii) they are not usually handled as a single object, but as populations of very large number of individuals (~ Avogadro number). These two unique characteristics make the definition of molecular chirality not as simple as that of a rigid object (such as a quartz crystal), and therefore it needs further developments in order to be refined [2].

The object molecule can be described at different levels of complexity, which are represented by models [3, 4]. The chemical formula, which uses atomic symbols for the atoms and lines for the bonds (traditionally, dashed lines for the weakest bonds), is no more than what has been termed a molecular graph, a concept derived from mathematics that has been introduced and used fruitfully in various areas of chemistry, in particular in molecular topology (see section 1.3). The structural formula is more informative because it shows the spatial relationships between the atoms and the bonds, which can be, for example, probed by nOe effects in NMR spectroscopy. The most accomplished description of the molecule as a rigid object is the 3D representation resulting from an X-ray crystal structure analysis, as it gives the distances between the atoms (bond lengths), and the angles between bonds. This points to the fact that the image of the molecule we have depends on the observation technique – in particular its timescale, observation conditions such as temperature, but also the state of the observed molecule (solid, solution, gas) [5]. In fact, a large number of molecules, including chiral ones, can be described using the approximation of rigidity (i.e., a rigid model) because fluctuations of atom positions are averaged around a thermodynamic equilibrium value at the observation timescale. In that approximation, as pointed out by Mislow [4], the chirality of the molecule is the chirality of the model, which depends only on the atomic positions, so that in principle the bonds can be ignored. However, the

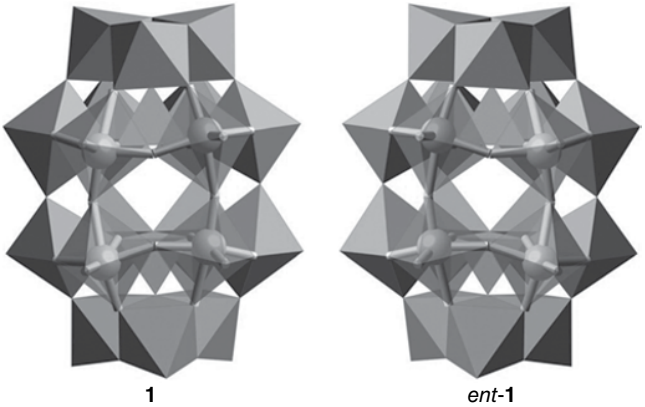

Figure 1.1 *The enantiomers of the chiral Keggin polyoxometallate α-$[P_2Mo_{18}O_{62}]^{6-}$* ***1****. The chirality of this molecule has a dynamic character, which allows the dynamic thermodynamic resolution of a given enantiomer of this hexaanion by interaction with enantiomerically pure cations*

presence of a bond between two atoms indicates that these atoms are closer to each other than if they were not bonded, so that, in practice the bond formalism is very useful for assessing, in a straightforward manner, the chirality of a rigid molecular model. This is the case where, for example, within two identical sets of atoms symmetry-related bonds have different lengths, leading to a distortion of the entire structure. Such an example of chirality due to alternating bond lengths is illustrated by the Keggin polyoxometallate α-$[P_2Mo_{18}O_{62}]^{6-}$ **1** of Figure 1.1 [6].

1.2.1 Origins and Description of Chirality within the Rigid Model Approximation

1.2.1.1 General Considerations

This section will deal with general considerations relating to the description and origins of chirality. Examples selected for their unique chirality properties will be then discussed in more detail in the following sections. Rigidly chiral molecules can only undergo rotations about bonds. They belong to one of the following point groups: (C_1, asymmetric), C_n, D_n, T, O, and I – the latter three being quite rare (see section 1.2.1.3) – which contain only proper symmetry axes as symmetry operations (Table 1.1). Molecular chirality concerns molecules or molecular assemblies featuring a 3D structure. The latter is determined by the interplay between molecular constitution, atom bonding geometry, and intramolecular and intermolecular interactions – including repulsions resulting from strain and steric hindrance. These factors then translate into arrangements of atoms that are either asymmetric (no symmetry element is present) or dissymmetric (with $C_{n>1}$ symmetry elements only) in the 3D space – the necessary but not sufficient (see below) criteria for chirality [2].

The conversion of a planar object into a 3D object can be achieved by either of two possible pathways. It is illustrated in Figure 1.2, starting from a rectangle as an example of a 2D object. Of course the rectangle, lying horizontally, is achiral (D_{2h} symmetry). In the first pathway let us take one of the points of the rectangle, for example its center, and pull

Table 1.1 *Symmetry elements of chiral point groups, the corresponding geometries they are generated from, and maximal symmetries*

Point group (achiral geometrical figure)	Symmetry elements	Symmetry properties
C_1 (general polyhedron)	None	Asymmetric
C_n, n≠1 (cone)	C_n	Dissymmetric
D_n, n≠1 (cylinder)	C_n, n × C_2	Dissymmetric
T (tetrahedron)	4 × C_3, 3 × C_2	Dissymmetric
O (octahedron and cube)	3 × C_4, 4 × C_3, 8 × C_2	Dissymmetric
I (icosahedron and dodecahedron)	6 × C_5, 10 × C_3, 15 × C_2	Dissymmetric

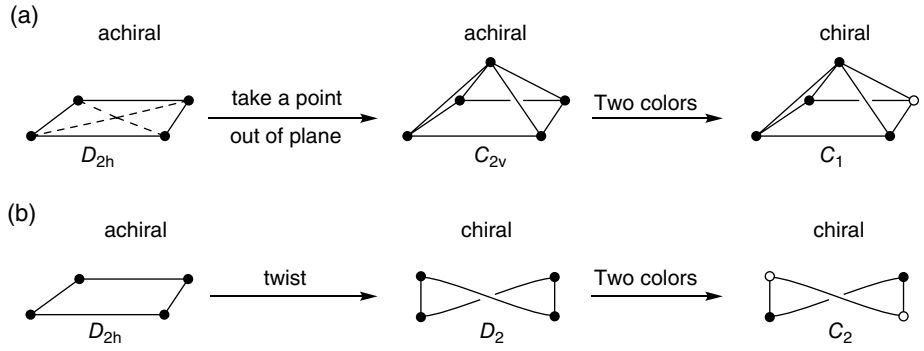

Figure 1.2 *Two pathways for the conversion of a planar object into a 3D object, exemplified by a rectangle. (a) Taking a point out of the plane of the rectangle generates an achiral C_{2v}-symmetric pyramid, of which the desymmetrization to a C_1-chiral object requires the use of two colored vertices (black and white). (b) Twisting converts the rectangle into a D_2-symmetric chiral object, the symmetry of which can be decreased to C_2 by coloring (black and white disks) of selected vertices*

it out of the plane along the vertical direction. This will generate a C_{2v}-symmetric pyramid. This achiral pyramid can be made chiral by changing its constitution – e.g. by coloring selected vertices: a minimum of two colors is required, as shown in Figure 1.2a, which produces an asymmetric (C_1) pyramid. The second pathway arises from a twist to the rectangle along its principal C_2 axis, which makes it a propeller with D_2 symmetry (Figure 1.2b). Hence, unlike the former case, the generation of chirality is simultaneous with the generation of a 3D object. Next, the symmetry is decreased to C_2 by color-differentiation of any two vertices out of the four. Of course, making three vertices of the same color would further decrease the symmetry of the propeller to C_1.

Stacks of an achiral planar object (such as an isosceles triangle, as shown in Figure 1.3) can produce an achiral D_{3h} symmetrical column (b), which upon a regular twist of the individual components is converted into a chiral wreathed column, either left- (a) or right- (c) handed.

In chemical vocabulary, the deformation applied to the rectangle of Figure 1.2a corresponds to a constitutional change as the rectangle (four vertices) has been changed to a

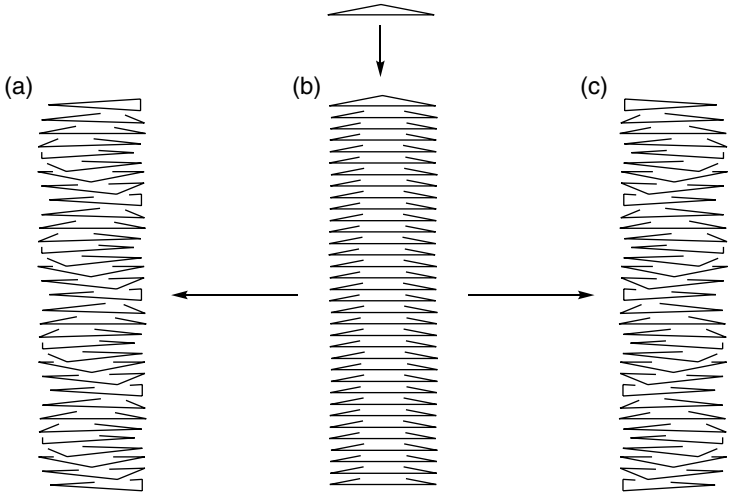

Figure 1.3 *Generating chirality by making (b) stacks of a planar triangular figure, followed by twisting of the resulting column either anticlockwise (a) or clockwise (c)*

pyramid (five vertices), whereas in the case of Figure 1.2b it corresponds to a conformational change as the twisted object has the same number of vertices and faces. Twisting may result from various mechanisms, such as rotations about bonds or variations in bond lengths – and in the case of molecular assemblies, from the generation of a curvature because of intermolecular attractions or repulsions.

The two basic processes of Figure 1.2 can be illustrated in the construction of the mirror-image molecular parallelepipeds $[Zn_2\text{-}\mathbf{2}]_4$ shown in Figure 1.4 by self-assembly of Zn(porphyrin) covalent dimers (*R*)-Zn_2-**2** and (*S*)-Zn_2-**2** driven by the Zn-pyridyl interaction [7]. The vertices of the cubes are occupied by Zn porphyrin (ZnPor) subunits, whereas four parallel edges are formed either by *meso* C–C single bonds or the *meso* C–(4-pyridyl)–ZnPor bond sequence. The bis(porphyrin) subunits are twisted by 90° with respect to each other, while each Zn^{2+} cation has a pyramidal N5 environment in the assembly.

The specification of chirality was formalized by Cahn, Ingold, and Prelog using (in the first instance) the "chirality model," which involves three stereogenic elements of chirality: the center, the axis, and the plane [8]. The chirality model of molecules is based on the tetrahedron, which is also the minimal 3D polyhedron [9]. In the first case (asymmetry, Figure 1.5) the perfect tetrahedron of T_d symmetry needs four different achiral vertices (A, B, C, and D) to be C_1 chiral (asymmetric constitution). Another possibility is to consider a tetrahedron of C_1 symmetry, in which all six edges have different lengths (asymmetric arrangement of the atoms). In practice, the asymmetric tetrahedron results both from asymmetric constitution and atom arrangement (Figure 1.5d).

In the second case (dissymmetry, Figure 1.6), elongation along one of the C_2 symmetry axes of the tetrahedron of Figure 1.5a decreases its symmetry to D_{2d}, and therefore only two different achiral substituents (A and B) are now needed to make it C_2-symmetric chiral. In addition, the D_{2d} elongated tetrahedron can also be made chiral without the need of substituents, by differentiating another pair of edges that are related by the main C_2 axis (z direction). This is done by compressing the tetrahedron of Figure 1.6a in the y direction,

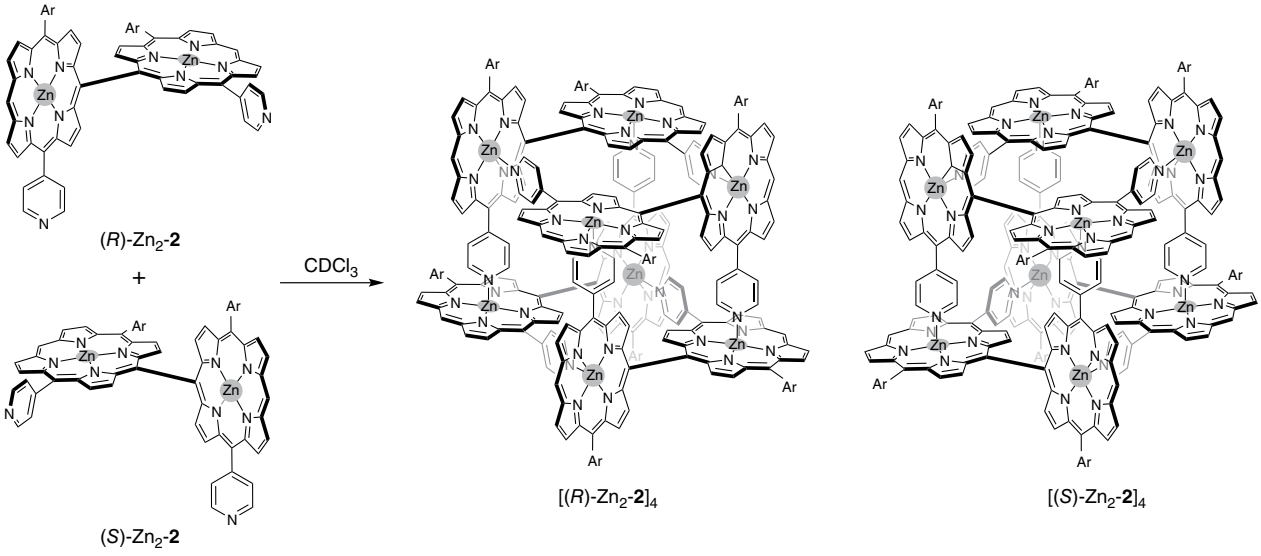

Figure 1.4 *Formation of homochiral assemblies [(R)-Zn_2-**2**]$_4$ and [(S)-Zn_2-**2**]$_4$ from twisted Zn(porphyrin) covalent dimers (R)-Zn_2-**2** and (S)-Zn_2-**2**, based on the Zn^{2+}-pyridyl interaction*

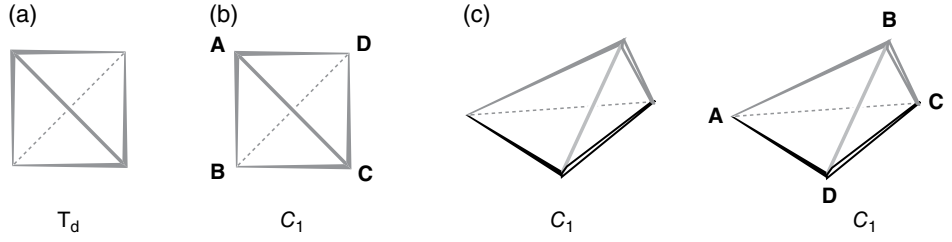

Figure 1.5 *Making the regular, T_d symmetric, tetrahedron (a) asymmetric: (b) by assigning the vertices four different labels; (c) by differentiating the lengths of all six edges using six different "colors"*

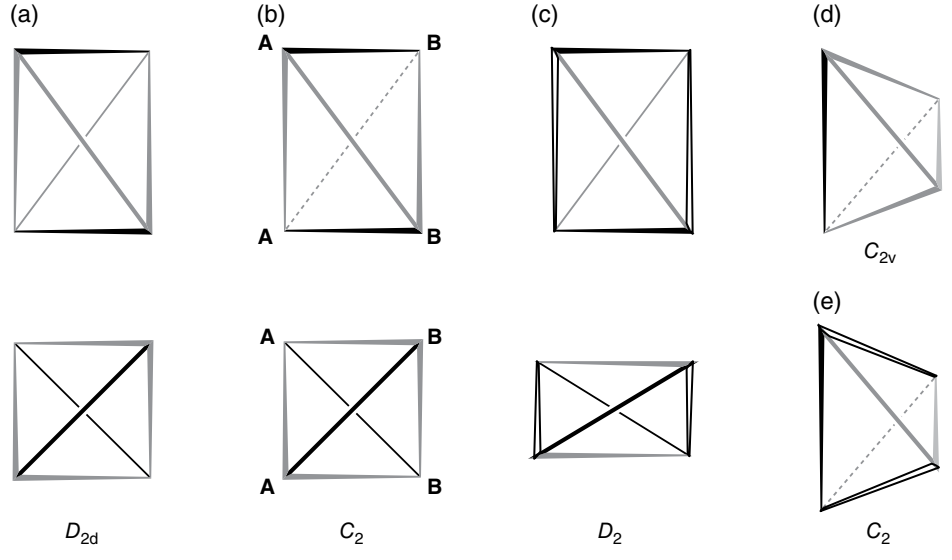

Figure 1.6 *Desymmetrization of the regular tetrahedron. (a) Elongation along one of the C_2 symmetry axes makes the two edges that are perpendicular to it (colored in black) different from the others. A view from the top is shown below the side view. (b) This D_{2d}-symmetric tetrahedron is made C_2-symmetric by labeling the four edges with two different labels, A and B. (c) It can be made D_2-symmetric by further coloring (in white) two edges that are symmetry related by the main C_2 axis. As shown in the top view below, this corresponds to a second elongation, along the C_2' axis. (d) The symmetry of tetrahedron (a) is further decreased to C_{2v} by differentiating a third edge (colored in light gray). (e) The latter is made C_2-chiral by coloring in white two edges that are related by the C_2 symmetry axis, leaving the two others in dark gray*

which removes its symmetry planes. The resulting tetrahedron (Figure 1.6c) is D_2-symmetric. Decreasing the symmetry of the D_{2d} tetrahedron further by moving symmetrically two vertices closer to each other as shown in Figure 1.6d, produces a C_{2v}-symmetric tetrahedron, which is made C_2-symmetric chiral by differentiating a pair of C_2 symmetry-related edges (Figure 1.6e).

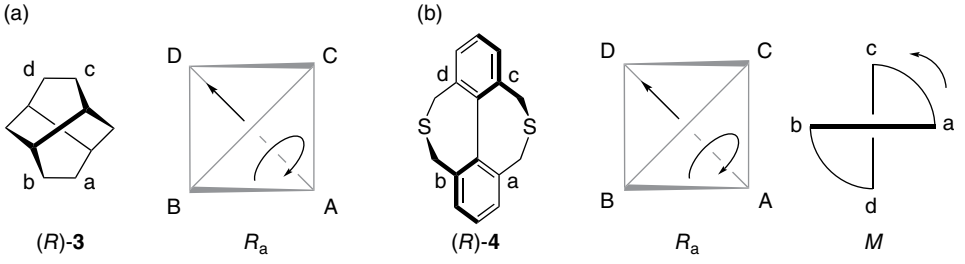

(*R*)-**3** R_a (*R*)-**4** R_a *M*

Figure 1.7 *Description of chirality using the chirality axis as stereogenic unit (a, b), and comparison with the description of chirality by identification of a twist (b). a) (+)-Twistane* ***3****. The chirality axis bisects [a, b] and [c, d]. b) A* D_2*-symmetric doubly bridged biphenyl* ***4****. The chirality axis is the biphenyl Ar-Ar bond. In both cases the positions of a and b are arbitrary, however the CIP rules govern those of c and d. Biphenyl (b) is also a molecular propeller, the conformation of which is* M

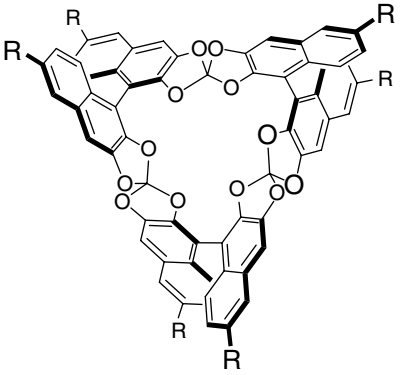

(*R*,*R*,*R*,*R*,*R*,*R*)-**5** (R = H or *n*Bu)

Figure 1.8 *The 3D triangular Janus cyclophane* ***5*** *is made by connecting three homochiral binaphthol-derived subunits by three carbon bridges. The configuration of all six chirality axes is* R

Figure 1.7 illustrates how two molecules, the 3D structures of which arise from different factors, are described using the same formalism (the chirality model) – in this particular case, the chiral axis. (+)-Twistane **3** (Figure 1.7a) owes its chirality to a highly symmetrical arrangement of sp^3 carbon atoms in space. The ansa-biphenyl **4** of Figure 1.7b is D_2-symmetric chiral due to strain-relieving twisting. Both molecules have the same configuration (R_a), which is obtained from the chirality model. In addition, the biphenyl can also be considered as a molecular propeller, and as its 3D structure is of conformational origin, it is best described using the *M*/*P* nomenclature. From the CIP rules, it is the *M* conformation that corresponds to the R_a configuration.

An additional illustration of the chirality axis is given in Figure 1.8, which shows a tris(spiroorthocarbonate) cyclophane (**5**) made in low yield by condensation of (*R*)-2,2′,3,3′-tetrahydroxy-1,1′-binaphthyl with dichlorodiphenoxymethane as the carbon source in refluxing toluene [10]. The resulting D_3-symmetric cyclophane has six chirality axes, three

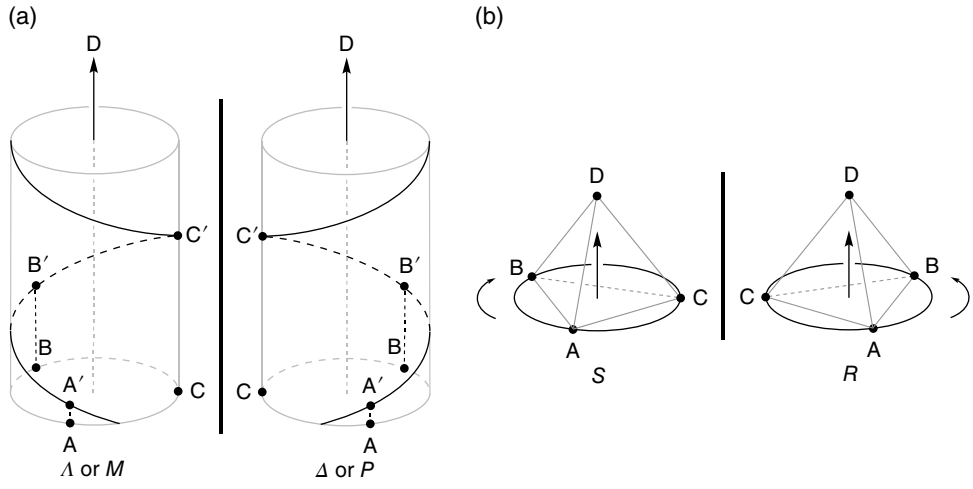

Figure 1.9 *Two different ways to define and orient the 3D space and the analogies between them. (a) Definition and orientation of the 3D space within the helicity model: generation of a helix and description of helical chirality using the Λ, Δ or* M, P *descriptors. (b) Chirality model: reduction of the stereogenic unit to a tetrahedron substituted with four different substituents (descriptors* S *and* R*). The vertical arrows are oriented towards the face from which the ABC plane must be seen. In (a) the D point has been sent to the infinite. Note that, when both models can be equally applied, there is no relationship between the helicity and chirality descriptors, except in the case of the biaryls, where* M *and* P *correspond respectively to* R *and* S

of conformational origin from the binaphthyl components, and three of configurational origin from the spiroorthocarbonate connections, which are interdependent. This molecule features two back-to-back aromatic concavities, which were shown by X-ray crystallography to be able to complex two C_{60} guests via multivalent π-π interactions.

The other model that was devised by Cahn, Ingold, and Prelog is the "helicity model," which proved subsequently to be extremely relevant in describing the chirality of a great variety of molecules and polymers, in spite of the fact that – at the time it was proposed – examples of helical nanoscale objects were rare [8]. From the mathematical viewpoint, a helix results from the combination of a rotation and a translation, and can be cylindrical (C_2 symmetry) or conical (C_1 symmetry). Once a helical structure is clearly identified, for example as a secondary structure, the sense of chirality is given by the helical path. If a clockwise rotation produces a translation away from the observer (following the sequence A′, B′, C′ in Figure 1.9a), the sense of chirality is *P* or *Δ*; if the same effect is produced by a counterclockwise rotation, the sense of chirality is *M* or *Λ*. Note that *P* and *M* descriptors generally apply to conformations and to the so-called secondary structures, and that the *Δ* and *Λ* descriptors are used for the configurations of transition metal complexes.

Natural macromolecular compounds such as DNA, polypeptides, and amylose, as well as synthetic examples such as polyacetylenes and polyisocyanates, can take up helical shapes [11]. This is also the case with molecular compounds like foldamers [12], helicenes [13], and helicates [14] (Figure 1.10). Larger structures encompass at least a full helix turn. By contrast, the smaller members of these families of molecules do not incorporate a 360° turn

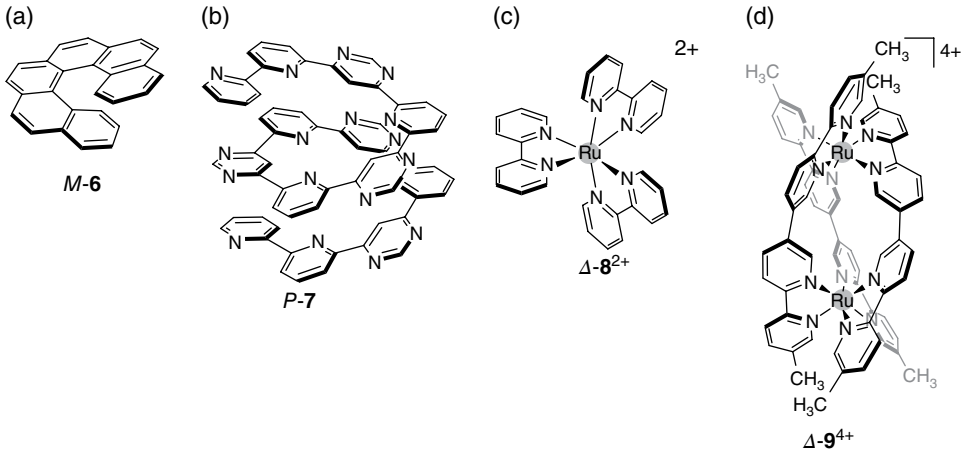

Figure 1.10 *Examples of helically chiral molecules and molecular propellers. (a) [6]Helicene* ***6****. (b) Foldamer* ***7*** *based on alternating pyridine and pyrimidine subunits. (c) The* $[Ru(bipy)_3]^{2+}$ *coordination complex (*$\mathbf{8}^{2+}$*), where bipy is 2,2′-bipyridyl, is a* C_3*-symmetric propeller. (d) Connecting two homochiral* $[Ru(bipy)_3]^{2+}$ *subunits through the positions 4 and 4′, respectively, of the bipy ligands produces a fragment of the triple helical dinuclear complex* $\mathbf{9}^{4+}$ *in which each quaterpyridine ligand has the same helical conformation*

and actually represent helical fragments: This is notably the case of the so-called molecular propellers [15] (Figure 1.10c), or of molecules that feature a simple twist (Figure 1.7b). Helicity can also manifest itself at the supramolecular level, for example in the case of helical stacks of achiral molecules. It is important to note at this stage that the formation of hierarchically organized chiral supramolecular structures can make the connection between nanoscopic and microscopic or macroscopic chirality (e.g., chiral molecular gels or chiral mesophases). The highest symmetry molecular propellers belong to the D_n symmetry point groups. Among D_n-symmetric propellers, those belonging to the D_2 symmetry point group are worth highlighting because they make the connection between the helicity model and the chirality model, as both models apply in that case (see Figure 1.7b).

As is the case for DNA, many helically chiral molecular compounds feature double or triple helices. This is particularly the situation for the helicates in which polychelate ligands take up helical conformations upon bridging at least two metal cations. This is illustrated in Figure 1.10d by the dinuclear Ru^{2+} complex of a quaterpyridine ligand ($\mathbf{9}^{2+}$) [16].

After this short overview of the origins and description of chirality we shall detail several examples that illustrate the two basic principles of formation of chiral structures in the 3D space shown in Figure 1.2 – that is, desymmetrization by constitution and desymmetrization by twisting.

1.2.1.2 Desymmetrization by Constitution

Figure 1.11 shows the grid-type tetranuclear metal-ligand assembly $[Os_2Fe_2(\mathbf{10})_4]^{8+}$ made from a "fused" bis(terpyridine)-like ligand (**10**) (in which two 2,2′-bipyridine moieties are bridged by a central pyrimidinyl fragment), and two different metal ions (Os^{2+} and Fe^{2+}),

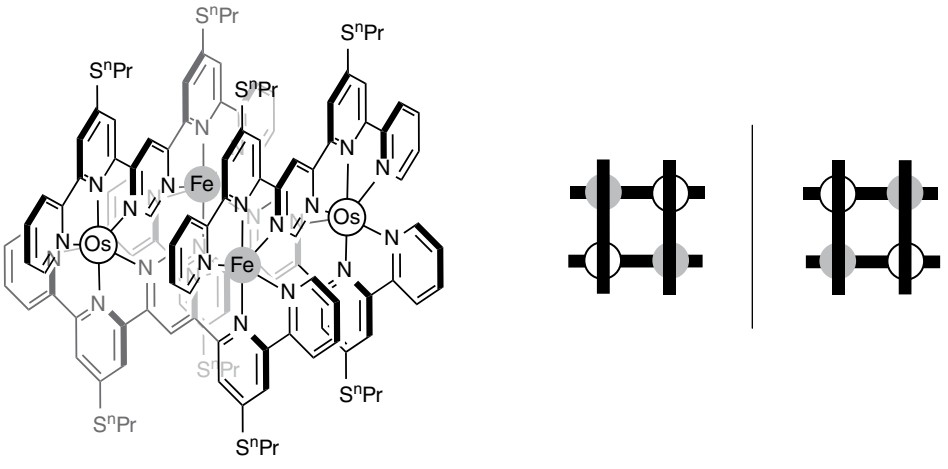

Figure 1.11 *The chirality of the grid-type tetranuclear complex $[Os_2Fe_2(\mathbf{10})_4]^{8+}$ of the "fused" bis(terpyridine)-like ligand* ***10***

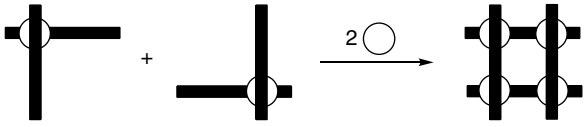

Figure 1.12 *The achiral D_{2h}-symmetric molecular grid is formed from two homochiral halves of mononuclear corner complexes with the bischelate ligands (black elongated rectangles) by addition of two metal cations that are identical to those involved in the starting homochiral complexes*

the pairs of identical metal centers being located on a diagonal [17]. This was done in a straightforward manner by introducing the metal centers in the order of increasing lability – reacting at first the di-chelate with NH_4OsCl_6 in 1 : 1 ratio, thus generating a corner-type chiral mononuclear complex, followed by the addition of $Fe(BF_4)_2$ (2 equivalents). Interestingly, the reaction proceeded stereoselectively to produce the chiral D_2-symmetric tetranuclear complex, as only corner-type precursors of the same handedness react with each other, excluding the formation of achiral *meso* C_{2v} assemblies. It is noteworthy that the tetra-homonuclear assembly represents a stereochemical curiosity, as it can be disconnected into two homochiral mononuclear di-chelate complex subunits. This illustrates the stereochemical paradox called "la coupe du roi" (Figure 1.12) [18].

Another remarkable case of desymmetrization by molecular constitution is offered by the higher order fullerenes. Fullerenes were unprecedented examples of molecules featuring a closed-shell structure. C_{60} itself has icosahedral I_h symmetry and is therefore achiral, but several higher order fullerenes such as $\mathbf{C}_{76}$, have been isolated and characterized. $\mathbf{C}_{76}$, which derives from C_{60} by incorporation of 16 additional C atoms, has D_2 symmetry, as shown by ^{13}C NMR (19 lines of equal intensity), and its chirality arises from its oblong,

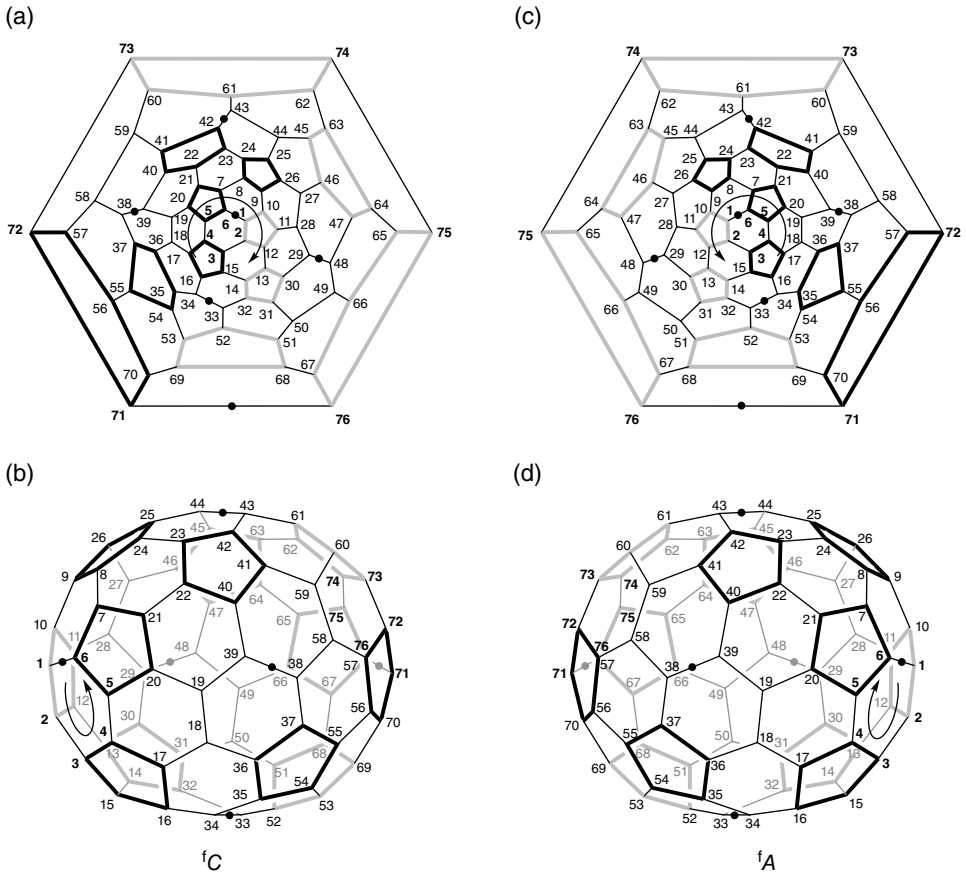

Figure 1.13 *Schlegel diagrams (a and c) and perspective representations (b and d) of the corresponding enantiomers of* $\mathbf{C}_{76}$*. The double bonds have been omitted for clarity. Five-membered rings have been highlighted in bold (black for the front ones, light gray for the rear ones in (b) and (d). The Schlegel diagram is obtained by opening the C71 to C76 six-membered ring and looking down the C1 to C6 analog (bold labels). The descriptor is* ^{f}C *if the C1 to C6 sequence is clockwise and* ^{f}A *if it is the opposite. The intersection of the three* C_2 *axes with the bonds have been materialized by the black dots: the vertical axis crosses C43–C44 and C33–C34, one horizontal axis crosses C1–C6 and C71–C76, and the other crosses C38–C39 and C29–C48*

helically twisted structure (Figures 1.13b to 1.13d) [19]. The enantiomers of $\mathbf{C}_{76}$ were resolved through the HPLC separation of the two diastereomers obtained by regioselective functionalization of $\mathbf{C}_{76}$ with an optically active malonate, followed by an electrochemical retro-Bingel reaction performed on each isolated diastereomer to release each optically pure $\mathbf{C}_{76}$. In principle, as all carbon atoms are pyramidalized, the configuration of the fullerene can be described by listing the absolute configuration (*R* or *S*) of each stereogenic center. The latter is obtained by developing the corresponding hierarchic directed graph which, however, is a cumbersome task.

Therefore a simplified procedure, which uses a single descriptor, has been developed which relies on the fact that the numbering schemes of fullerenes are helically chiral (Figures 1.13a to 1.13c), and can be used to differentiate between enantiomeric fullerenes. Whereas two isometric mirror-symmetric numbering schemes can be applied to an achiral parent fullerene such as C_{60}, a unique one is associable with a specific enantiomer of an inherently chiral carbon spheroid. Depending on whether the path traced from C(1) via C(2) to C(3) of this numbering is clockwise (C) or anticlockwise (A), the descriptors are defined as ^{f}C and ^{f}A. Figures 1.13a and 1.13c show the Schlegel diagrams of the enantiomers of $\mathbf{C}_{76}$ viewed through the opening of the six-membered C71–C72–C73–C74–C75–C76 cycle in the direction of its C1–C2–C3–C4–C5–C6 analog. The sense of the latter sequence (clockwise or anticlockwise) gives the chirality descriptor ^{f}C or ^{f}A. As $\mathbf{C}_{76}$ is D_2-symmetric, it has three C_2 symmetry axes that are orthogonal to each other.

Concave, bowl-shaped molecules represent a very important family of receptors and precursors of receptors that may display chirality [20]. Examples are resorcinarenes, calixarenes, cyclotribenzylenes and cyclotriveratrylenes, tribenzotriquinacenes [21], sumanenes [22], subphthalocyanines [23] and receptors built from these compounds – such as the cryptophanes made by dimerization of functionalized cyclotribenzylenes [24], or molecular capsules assembled by hydrogen bonding between urea-functionalized calix[4]arenes [25]. As concave molecules are nonplanar, they can be made chiral just by rim orientation. The simplest geometrical model of a concave molecule is a tetrahedron with an "empty" ABC face opposed to the D vertex [26]. Calix[4]arenes carrying at least two different substituents in the *para* positions of the phenol rings, or having even a single *meta* substituent, such as **11** (Figure 1.14a) [27], cryptophanes carrying two different substituents at the *meta* positions of the phenylene rings, such as **12** (Figure 1.14b) [24] – just to mention a few – are examples of concave molecules that owe their chirality to rim orientation. These compounds have been qualified as "inherently chiral," because their chirality (which does not depend on the presence of chiral substituents) is a property of the overall structure [26]. However, this expression may be misleading as bowl inversion, when it is possible, reverses the sense of chirality: therefore concave molecules are better described under the heading of conformational chirality [28]. The recommended descriptors to characterize these molecules are *P* and *M* [8]. Rim orientation of achiral concave molecules may also result from the concerted orientation of substituents, for example by a directed network of hydrogen bonding. The self-assembled molecular capsule $(\mathbf{13})_2$ of Figure 1.14c is obtained by Et_4N^+-templated head-to-head dimerization of two urea-substituted calix[4]arene (**13**) components [25].

Cyclodextrins are concave macrocyclic oligomers of *D*-glucose, and are therefore enantiomerically pure compounds. The recent development of efficient methods for the selective functionalization of their primary rim has led, in particular, to the synthesis of α-cyclodextrins carrying three different substituents [29]. Figure 1.15 shows an example in which the original primary alcohol functions have been replaced by $-PPh_2$, -OBn (Bn is CH_2Ph) and -Me groups that alternate twice, which imparts an orientation to the primary rim. Therefore, the modified cyclodextrin has two diastereomers **14a** and **14b**, because the chirality due to rim orientation is superposed on the chirality of the native cyclodextrin backbone. The resulting molecule can be considered a diphosphine ligand, and indeed it was used in the Tsuji–Trost allylation reaction. It was shown that opposite orientations of the primary rim led to opposite enantioselectivities, albeit rather low (30%), whereas the

(a)

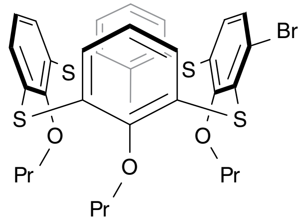

M-**11**

(b)

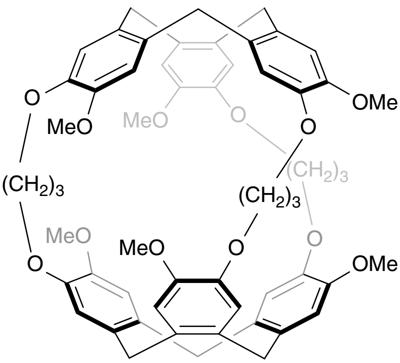

P-**12**

(c)

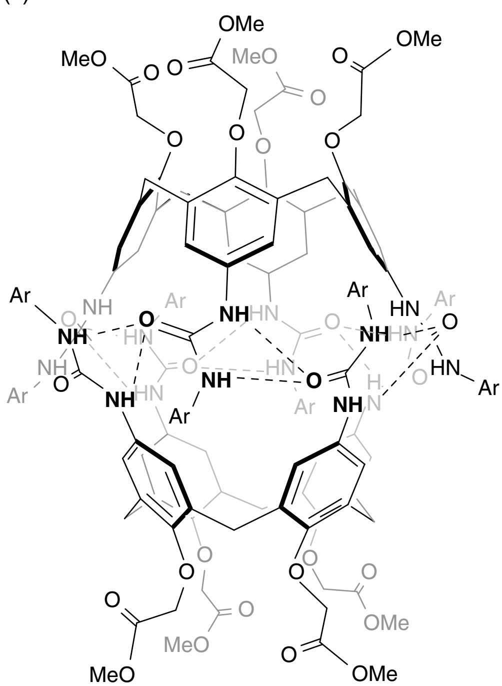

Et_4N^+@(**13**)$_2$

Figure 1.14 *Examples of concave chiral molecules. (a) One of the phenyl rings of thiacalix[4]arene* ***11*** *bears a bromine atom in the* meta *position, which destroys the* C_{4v} *symmetry of the parent compound, and makes the corresponding system asymmetric. The propyl groups prevent ring inversion at ambient temperature. (b) Cryptophane-A (**12**) in the chiral,* anti-*configuration* (P). *(c) A head-to-head calix[4]arene dimer (**13**)$_2$ via hydrogen bonding between arylurea substituents, that encapsulates EtN*$^+$ *(removed for clarity; Ar*=p-*tolyl). The methyl acetate substituents maintain the macrocycles in the cone conformation*

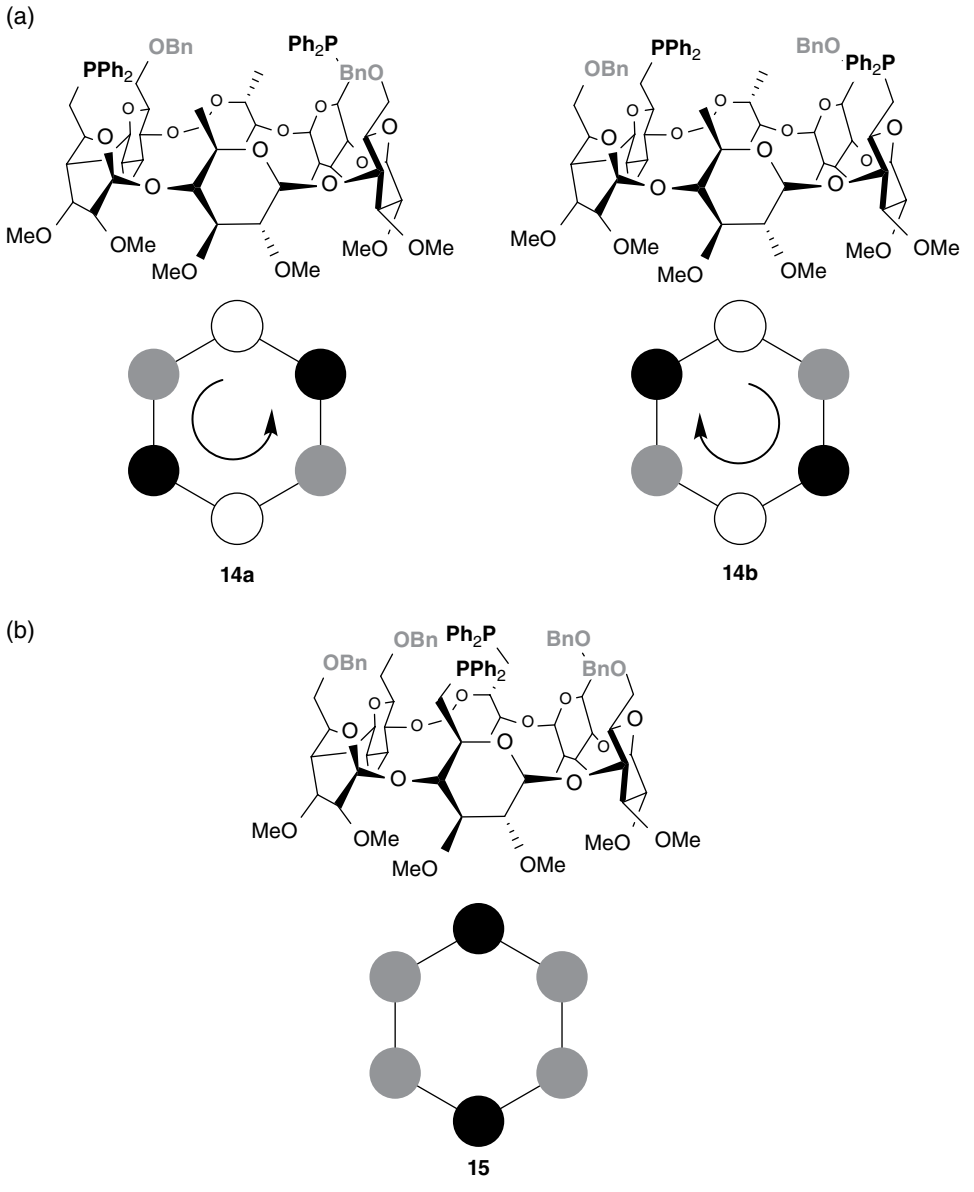

Figure 1.15 *Examples of (a) a pair of diastereomeric α-cyclodextrins (**14a** and **14b**) that differ by the primary rim orientation; (b) Cyclodextrin **15** is chiral; however, the primary rim is not oriented*

corresponding cyclodextrin (**15**) with a σ_h-symmetrical arrangement of two -PPh_2 and four -OBn groups led to no asymmetric induction at all. This pointed to the higher asymmetric character, with respect to the palladium-catalyzed allylation reaction, of the rim orientation by comparison with the cyclodextrin cavity.

1.2.1.3 Desymmetrization by Twisting

Examples of synthetic molecules exhibiting helical chirality are multidecker systems (cyclophanes, etc.) [30], helicates[14] or foldamers [12]. Whereas helicity of multidecker molecules results from constitutional features only, helicity of helicates and foldamers also involve intramolecular interactions as a twisting factor. Helicates are transition metal complexes containing at least two metal centers, and generally feature double- and triple-helical structures, single-helical cases being best described as foldamers. Helical folding of the multichelate strands is directed by the metal centers, the coordination geometry of which orients the ligands in well defined directions of space. Helicates containing at least two metals centers are linear but higher order helicates can show also circular [31] and other geometries, in particular tetrahedral, when they are made of four metal centers that occupy the vertices of a tetrahedron [32]. True helicates are chiral species that incorporate homochiral metal complex subunits. However, they can have diastereomers that differ by the sense of chirality at the metal centers. For example, in the case of dinuclear systems, there are two diastereomers, the enantiomeric pair of helicates (Δ,Δ and Λ,Λ), and the achiral, so-called mesocate (Δ,Λ), containing metal complex subunits that have opposite chirality senses. The formation of a helicate versus a mesocate has been shown to be highly dependent on the nature of the bridge and the connections between the chelates forming a polynucleating ligand strand – in particular *meta*-phenylene bridges strongly favor the helicate. This highlights the role of the ligand bridges in conveying the chiral information between stereolabile metal centers. Figure 1.16 shows two of the three possible diastereomers (excluding enantiomeric pairs) of the tetranuclear Fe^{2+} complex $[Fe_4(\mathbf{16})_6]^{8+}$ with a binucleating diimine ligand (**16**) built *in situ* from the corresponding amine and aldehyde, and bridged by a *p*-terphenylene spacer [33]. All four iron centers have the same chirality in the true helicate, which displays chiral *T* symmetry, whereas the *meso* form, incorporating two Δ and two Λ centers, has achiral S_4 symmetry. In the *T* isomer chelates of the same ligand display the *anti* orientation with respect to each other, and the three phenyl groups of the spacer are arranged with a helical twist that allows for the perfect stereochemical coupling between the metal centers, whereas in the case of the S_4 isomer four of the six bridging ligands have the *syn* orientation.

The diastereomeric ratio of the *T*, S_4, and C_3 diastereomers was ca. 1 : 1 : 1. However, it could be changed by modification of the terphenyl spacers connecting the diimine ligands. The *anti* orientation is favored by introduction of two methyl substituents *ortho* to the central ring, which induce a 60° dihedral angle between adjacent phenyl rings, as a result of a weak van der Waals interaction between the methyl group and the phenyl group of an adjacent ligand [33]. The *syn* orientation is favored by constraining the two phenyl rings attached to the chelate groups to be parallel to each other. This is done by permethylation of the central phenyl ring, which makes it perpendicular to the peripheral rings. Therefore, when dimethylated terphenyl spacers are used, the major diastereomer is the true helicate (*T*-symmetry), whereas when tetramethylated terphenyl spacers are used, the major diastereomer is the *meso* form of S_4 symmetry. Stereochemical coupling between the metal centers is increased in the first case, whereas it is decreased in the second case.

Foldamers are single stranded molecules that can fold in order to take up directed bent conformations. Helicity is the conformational response to avoid steric interactions between overlapping sections of strands. In the case of the helicenes (Figure 1.10a), folding is encoded in the molecular constitution but in true foldamers it is the result of (programmed)

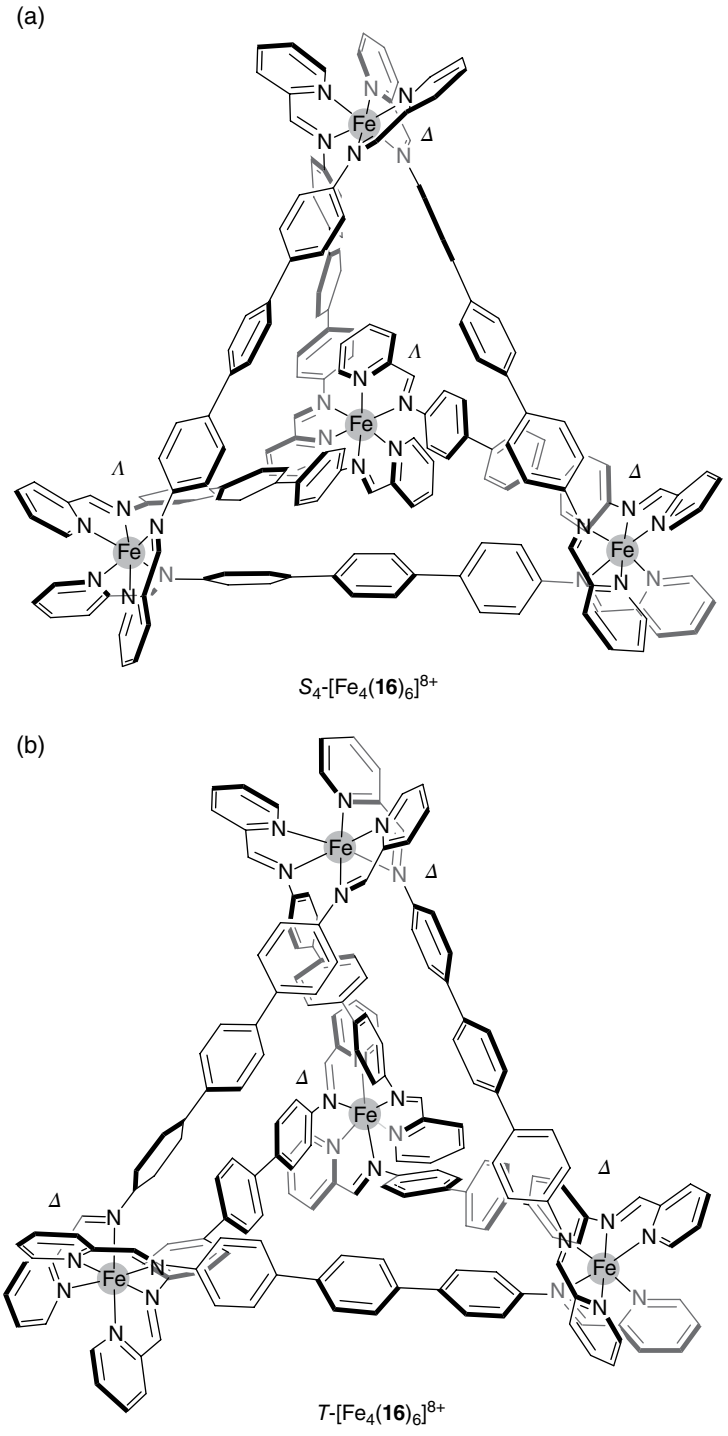

Figure 1.16 *Two diastereomers of the tetranuclear transition metal aggregate* $[Fe_4(\mathbf{16})_6]^{8+}$ *built on four* Fe^{2+} *cations and six binucleating diimine ligands* ***16****. (a) Achiral (Δ, Δ, Λ, Λ)* meso *form, with* S_4 *symmetry. (b) Chiral (Δ, Δ, Δ, Δ) form, with T symmetry*

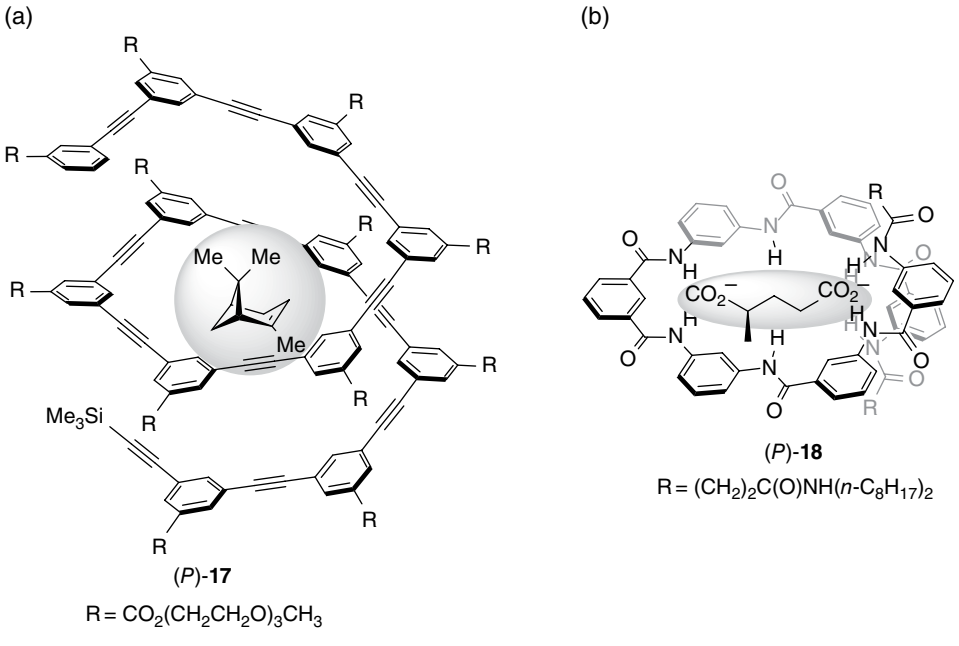

Figure 1.17 *Examples of foldamer hosts, the chirality sense of which is controlled by the chirality sense of the chiral guest. The preferred* P *conformation of the foldamers shown are controlled by (a) (–)-α-pinene in its complex with* ***17****, and (b) D-glutamate in its complex with* ***18***

intramolecular interactions – such as electronic repulsions (Figure 1.10b) or electronic attractions, and hydrogen bonding. When the strand wraps around a molecule, a cation or an anion, folding is the result of intercomponent interactions (such as van der Waals interactions), coordination bonds, and hydrogen bonds. Figure 1.17 shows two representative examples of foldamers that act also as hosts. The arylethynyl system **17** of Figure 1.17a folds around the neutral optically active (–)-α-pinene template [34] as a result of van der Waals and hydrophobic interactions, whereas the oligoarylamide system **18** of Figure 1.17b folds around the optically active D-glutamate dicarboxylate [35] as the result of hydrogen bonding interactions between the amide protons and the anionic carboxylate functions. Foldamers are in general dynamic systems. In the present cases the helicity sense of the foldamers is controlled by the absolute configuration of the optically active guest.

1.2.2 Dynamic and Supramolecular Chirality

1.2.2.1 Enantiomerization Pathways

There are molecules that can encompass enantiomeric conformations under the conditions of observation, and it is this very point that makes molecules unique nanoscale objects. Two cases can be distinguished, depending on the sequence of intermediates that are involved in the interconversion pathway, as they can involve achiral or only chiral species. The first case is classically illustrated by *cis*-1,2-difluorocyclohexane (**19**), the stable chair conformations of which have C_1 symmetry with one fluorine atom in equatorial position

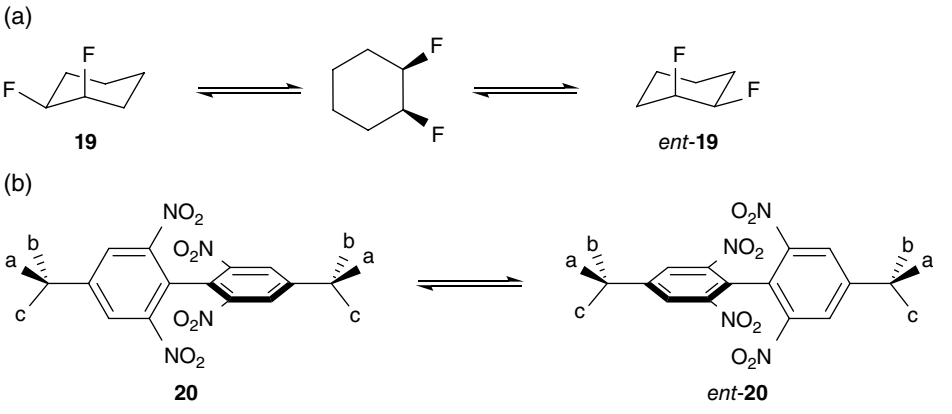

Figure 1.18 *(a) Interconversion of the asymmetric chiral conformations of* cis-*1,2-difluorocyclohexane* ***19*** *to their mirror-image involves an achiral intermediate of C_s symmetry. (b) The generic biphenyl* ***20*** *is chiral-asymmetric in all of its conformations. As a result, interconversion of mirror-image conformations takes place through a chiral pathway. Note that Cabc stands for the menthyl group*

and the other in axial position. Interconversion involves a higher energy achiral intermediate with C_s symmetry (Figure 1.18a). Other examples are provided by the mechanisms of racemization of octahedral transition metal complexes with bidentate ligands – i.e. the Bailar and the Ray–Dutt twists, which involve achiral trigonal prismatic species of D_{3d} and C_{2v} symmetry as intermediates, respectively. The second case is illustrated by the biphenyls of generic formula shown in Figure 1.18b (**20**) [36]. These molecules, composed of three rigid blocks (A, B, and A*; A* being mirror-image of A), are asymmetric in every conformation, because the symmetry plane exchanging A and A* is destroyed by the biphenyl block B. However, unrestricted rotation between the blocks A and B on the one hand, and B and A* on the other hand, allows for the smooth interconversion between mirror-image conformers without involving achiral intermediates. Such molecules mimic, at the nanoscale level, the reversal of a real rubber glove by peeling it off inside out from the hand. At no time during the process of interconversion does the glove achieve a shape with a symmetry plane. Molecules mimicking this process have later on been coined "molecular rubber gloves." The chirality of *cis*-1,2-difluorohexane can be detected by ^{19}F NMR spectrometry at low temperature, where the exchange of mirror-image conformations through the achiral intermediate is blocked.

Molecular rubber-glove molecules are important milestones in stereochemistry, because they can be used as the basis to express the sufficient condition for chirality: if a molecule is chiral, then there are no enantiomerization chiral pathways converting an enantiomer into its mirror image [2].

1.2.2.2 Controlling Chirality by Coordination and Supramolecular Interactions

In this section we consider molecules that are not rigidly chiral but can exist in the form of enantiomeric conformations, which are in the fast exchange regime under observation conditions (stereochemical lability). Such molecules are interesting platforms to elicit

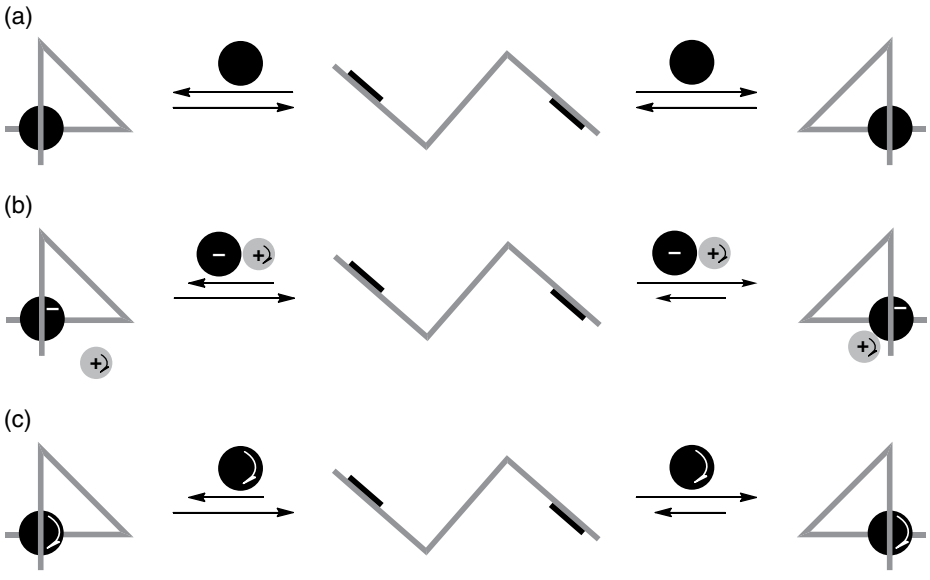

Figure 1.19 *Principle of freezing chirality by supramolecular or coordination interactions. A ditopic (black rectangles) linear receptor (central Z shape) can wrap around (a) an achiral guest (black disk) either clockwise (left) or anticlockwise (right). (b) If the guest is a charged species (e.g. an anion), the use of an optically active counter-ion (a cation) can lead to the control of host chirality by supramolecular ion-pair interactions. (c) The same result is obtained by using an optically active guest itself*

evidence of induced circular dichroism effects, to design chirality switches and molecular systems for chirality sensing (stereodynamic chemosensor), just to mention a few applications.

In order to control the chirality of a stereochemically labile molecule it is necessary to have an optically active chirality effector, which is able to interact with the former via supramolecular (e.g., hydrogen bonding, ion pair or van der Waals contact) or coordination interactions. Three cases of interest are reported schematically in Figure 1.19. Figure 1.19a represents the general case in which the achiral receptor, featuring two recognition elements, coils around an achiral guest. Assuming that the host-guest systems are in thermodynamic equilibrium, Figures 1.19b and 1.19c show two different approaches in order to control the sense of coiling of the host – either (Figure 1.19b) by using a ionic achiral guest in combination with an optically active counterion, or (Figure 1.19c) by using an optically active guest.

The phenomenon was independently described in the 1930s for the interaction of stereolabile transition metal complexes with optically active counterions by Pfeiffer [37] and Kuhn [38], who called it "asymmetric transformation." Most recent applications concern the design of receptors featuring chiral conformations, which can bind optically active guests. As a result, the dynamic equilibrium between diastereomeric host-guest pairs is biased towards the formation of the most stable one. Best evidence for the phenomenon was provided by induced circular dichroism. Figure 1.20 shows one of the numerous examples of the

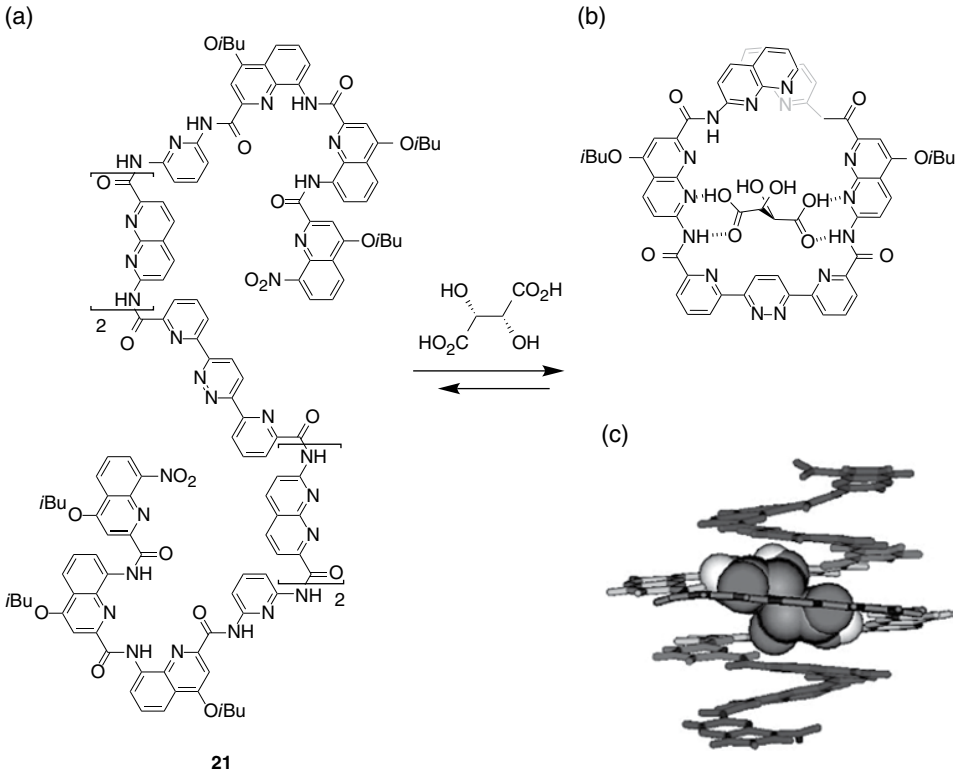

Figure 1.20 *Compound **21** (a), made of rigid aromatic hydrogen bond acceptors separated by carboxamide connectors, folds in a doubly conical, singly helical structure that features (b) a cavity able to host L-(+)-tartaric acid, as shown by (c) the view of the X-ray crystal structure. When the guest is optically pure, the diastereomeric purity of the host-guest ensemble is greater than 99%*

literature [39]. A foldamer (**21**) made of three different sequences symmetrically attached at the extremities of a central bis(pyridyl)pyridazine spacer forms a D_2-symmetrical bis-conical helical structure in $CHCl_3$/DMSO 98.8 : 0.2 v/v. This compact helical conformation features a central cavity, which is able to encapsulate various H-bond donor guests, such as L-(+)-threitol or L-(+)-tartaric acid (Figure 1.20). The latter, which shows the highest association constant ($5300\,M^{-1}$), also produces the stronger chiral bias, as the diastereomeric excess is greater than 99%.

1.2.2.3 Memory-of-Chirality Effects

Another related phenomenon is the "memory of chirality" effect, for which there has been evidence in the case of many achiral polymers that feature chiral helical conformations, such as polyacetylenes [40]. In addition, as we shall see in the next paragraph, this phenomenon is also frequently observed in the case of self-assembled helically chiral assemblies of molecules [41], but seldom in the case of small molecules. In the example

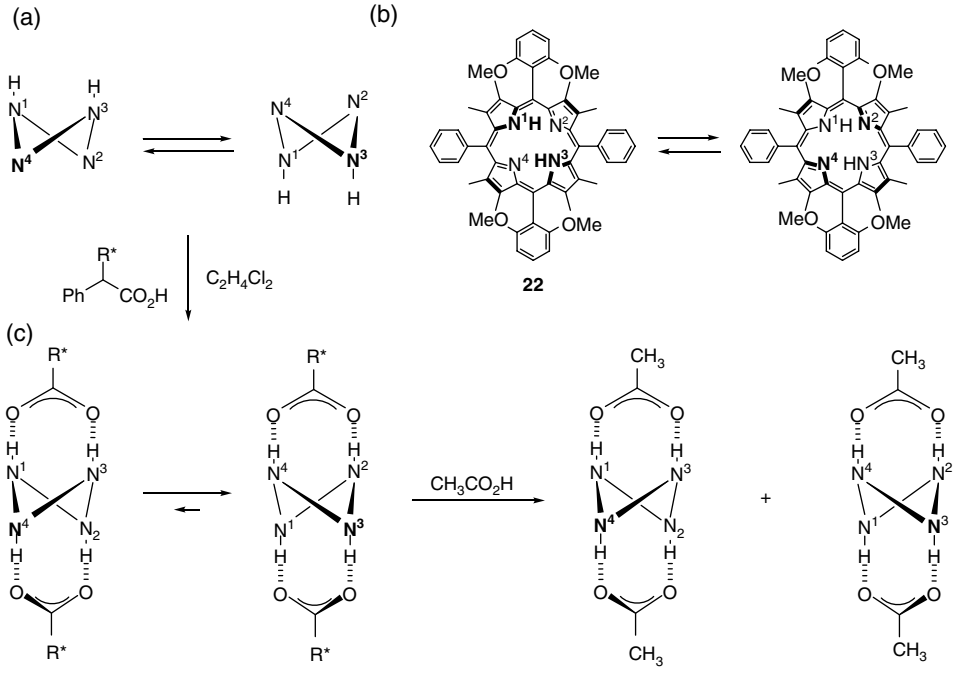

Figure 1.21 *Illustration of the chiral biasing of the equilibrium between mirror-image conformations of the ruffled porphyrin* ***22*** *depicted in (b). (a) Schematic view of the real system. (c) Addition of one equivalent of optically pure mandelic acid shifts the conformational equilibrium towards the formation of the most stable diastereomer. Replacement of mandelic acid by acetic acid, which is achiral, keeps the enantiomeric bias: this is the so-called memory-of-chirality effect*

shown in Figure 1.21 a sterically crowded porphyrin (**22**) has ruffled enantiomeric conformations in a 1 : 1 ratio. Binding of optically active carboxylic acid (host/guest = 1 : 2) by salt-bridge formation shifted the equilibrium to the most stable diastereomer (98% *de*), giving rise to an induced circular dichroism (ICD). Subsequently, the optically active carboxylic acid analyte was displaced by achiral acetic acid. The memory-of-chirality effect stems from the fact that there is no exchange between the acetic acid molecules bound to the hosts. As a consequence, two enantiomers (a major one and a minor one) are obtained. Remarkably, the ICD measured for the pair of enantiomers ($t_{1/2}$ = 200 h at 23 °C) is higher than the one measured for the pair of parent diastereomers [42].

Memory-of-chirality effects are actually more commonly observed in the case of chiral polymers. These are polymers taking up helical conformations, for example polyacetylenes, polyamides and polyisocyanates. Figure 1.22 shows schematically the experiments that could be carried out using a poly(aryl)acetylene carrying carboxylic acid functions [40]. The polymer takes up random-coil conformations that show domains with a well defined helical sense that are separated by reversal points. The polymer can be further functionalized by salt bridge formation with an optically active amine, which triggers the

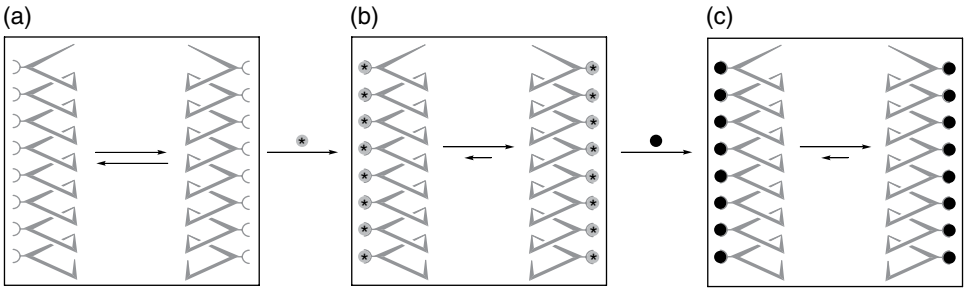

Figure 1.22 *Control of the chirality of polymers taking up helical conformations (a) by supramolecular interactions. The polymer contains appended binding groups, which upon interaction with a chiral, optically active guest (gray disks marked with a star), allow the control of the chiral bias between the mirror-image polymeric helices (b). (c) The memory-of-chirality effect takes place upon exchange of the chiral guest by an achiral analogue (black disks)*

homogenization of the favored chirality sense. The memory-of-chirality effect takes place upon exchange of the optically active amine for an achiral one.

1.2.2.4 Supramolecular Chirality

Supramolecular chirality must be distinguished from the previous cases, as it does not concern the chirality of an isolated molecule but the chirality of molecular assemblies constructed from achiral molecules held by noncovalent interactions (hydrogen bonding, coordination bonds, π-π stacking, dipole-dipole interactions, etc.) – such as aggregates of various shapes (in particular rods and ribbons), liquid crystals, solvent gels, and supramolecular polymers that are in dynamic equilibrium. The manifestation of supramolecular chirality is the formation of helical structures (see Figure 1.3), and these are characterized by circular dichroism. Remarkable phenomena have been observed (Figure 1.23). Chiral supramolecular polymers assembled from achiral molecular subunits (monomers) exist as racemates. Addition of an optically active chirality inducer (either a chiral version of the monomers, or a chiral molecule that is able to interact with the monomers) can bias the original equilibrium between the enantiomeric supramolecular polymers by formation of diastereomeric supramolecular polymers [41]. This phenomenon is a manifestation of the sergeant-and-soldiers principle, which was formulated for the first time in the case of covalent polymers made of achiral monomers plus a small amount of an optically active "dopant" [43]. The chiral "sergeant" molecule can be removed, without significantly altering the enantiomeric ratio between the mirror-image helices, because of kinetic effects. This is a manifestation, at the supramolecular level, of the memory-of-chirality effect [44].

Another chirality principle that was discovered in the case of covalent polymers, which also applies to supramolecular chirality, is the majority rule [45]. This rule applies when supramolecular polymerization uses only optically active chiral monomers. If an optically pure monomer is used, then an optically pure helical aggregate is obtained. However, if a racemate plus a slight excess of one of the enantiomer monomer is used, the majority rule tells us that the major supramolecular helical aggregate will be the one whose sense of chirality is dictated by the optically active monomer that is in excess [46].

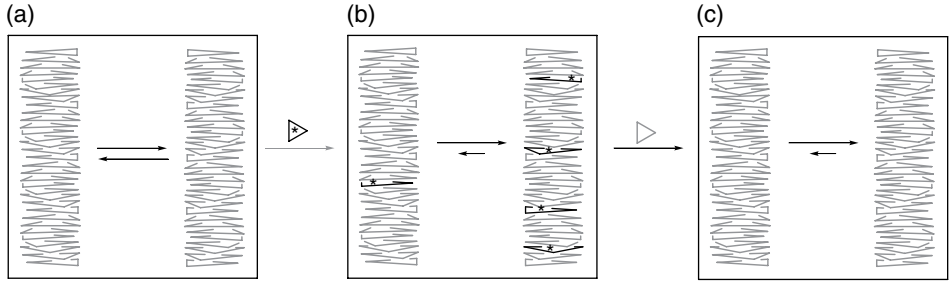

Figure 1.23 *Sergeant-and-soldiers principle in supramolecular chirality. (a) Aggregation of certain "soldier" achiral molecules (symbolized here as triangles) can lead to helical supramolecular structures held by π-π stacking or hydrogen bonding interactions. (b) Introduction of a small percentage of chiral, optically active monomer ("sergeant," starred triangle) leads to biasing of the ratio between the left- and right-handed supramolecular helices. (c) The "sergeant" molecules are replaced by equilibration with an excess of "soldier" molecules (grey triangle) without significantly changing the ratio between mirror-image stacks*

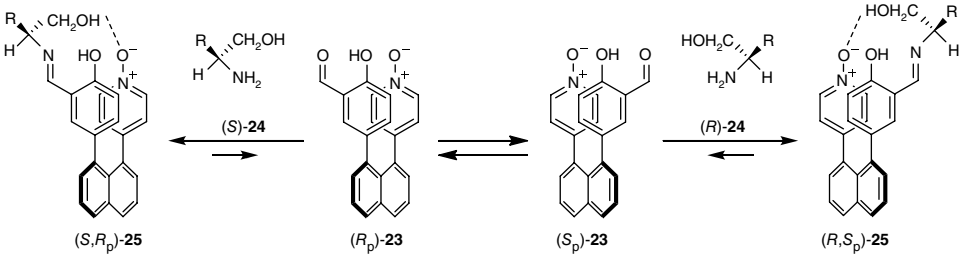

Figure 1.24 *A chemosensor (**23**) for chiral aminoalcohols based on a planar chiral naphthalene platform carrying a salicylaldehyde recognition subunit and a pyridine oxide chromophore*

1.2.2.5 Chirality Amplification and Switching of Chirality

The main consequence of dynamic chirality is the possibility of observing chirality amplification, because that chirality – be it of conformational or supramolecular origin – is never frozen once and for all. Chirality amplification translates into enhanced CD effects upon going from the optically active chirality inducer to the host-guest complex with the achiral receptor, because the latter may contain chromophores that are strongly CD active in a chiral environment [47]. As a consequence, the so-called induced circular dichroism (ICD) effect has been used as a principle of design for chirality sensors. Figure 1.24 shows one of numerous examples, in which a chiral aminoalcohol freezes out the enantiomeric conformations of a 1,8-diarylnaphthalene chromophore (**23**), by covalent and hydrogen bond formation between the analyte and the sensor [48]. In the case of supramolecular assemblies, positive nonlinear effects have been measured between the enantiomeric purity of the chiral dopant and the ICD of the assembly. Formation of supramolecular species (aggregates) could also explain nonlinear effects in asymmetric catalysis [49].

Chirality switching is not limited to molecular recognition and sensing. In some instances it has been induced by light irradiation [50] or solvent changes [51].

Finally, the phenomenon of supramolecular chirality resides at the interface between chirality at the nanometer level and chirality at the micrometer, if not millimeter, level. It is important to recall, in this respect, that it was the dissymmetric external shape of crystals of potassium tartrate examined with a microscope that suggested to Louis Pasteur that it could result from dissymmetric arrangements of the atoms of the salt. Hierarchical effects in chirality are observed in other materials than crystals. For example molecules forming liquid crystals can be combined with small amounts of chiral dopants that induce optically active liquid crystalline phases [52]. Similarly achiral molecular gelators can be doped with optically active analogs, leading to optically active solvent gels [53].

1.3 Topological Chirality

The chirality of a molecular object in the rigid geometry approximation is a property of the whole object, therefore it depends only on the positions of the atoms. This means that the bonds can be ignored, as first noted by Mislow [4]. This is exactly the opposite to the case of the topological character of chirality, which is invariant whatever the atomic positions, provided that all the connections (chemical bonds) between the atoms have been identified [3].

Molecular rigidity results from the stereochemical properties of atoms and bonds, from steric hindrance and strain, which limit the amplitude of bond rotations and elongations that could convert an enantiomer into its mirror image. It is at the very origin of geometrical chirality. There are cases, however, for which molecular rigidity is not a requirement for chirality, the molecule remaining chiral whatever the deformations – provided that no bonds can pass through each other. This is actually another form of molecular rigidity, which arises from topological constraints rather than geometrical ones. This section will focus on the concept of topological chirality, which, judging from the literature, has been somewhat overlooked.

1.3.1 The Molecular Graph

A graph G is an ordered pair (V, E) formed by a set of vertices V and a set of edges E connecting them. It is an abstract mathematical (topological) object; however, it can be embedded into and manipulated in 3D space. Whereas a geometrical figure is rigid and characterized by distances and angles, the embedded graph is endowed with complete flexibility: the vertices can be placed anywhere in space and the edges can be stretched or shrunk at will, the only requirement being that no two vertices can coincide and no two edges can cross each other – that is, edges and vertices represent boundaries that cannot be crossed. Embedded graphs in 3D space can be represented as a projection (the so-called presentation) in two dimensions, in which the relative positions of the projected edges (above or below) must be indicated [3]. Figure 1.25 shows different presentations of the $K_{3,3}$ graph, the so-called bipartite graph on three vertices, of which two are chiral. The topological property of $K_{3,3}$ is that it is a nonplanar graph – that is, it cannot be presented in the plane without any crossing. Examples of minimal presentations (a single crossing) are shown in Figure 1.25b and Figure 1.25c.

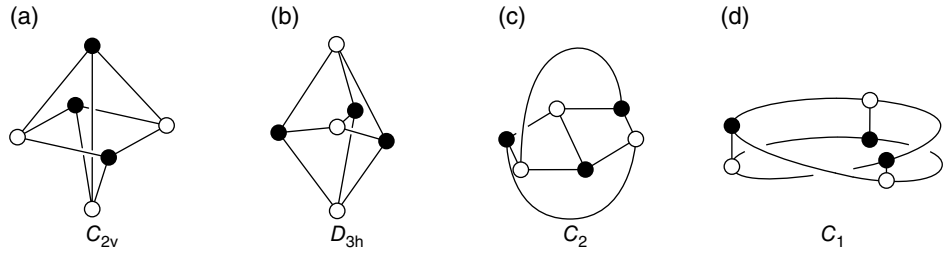

Figure 1.25 *Four presentations of the* $K_{3,3}$ *graph (the bipartite graph on three vertices) with their symmetry group. The presentations shown in (c) and (d) are geometrically chiral*

As the *graph of a molecule* is the set of atoms (vertices) and bonds (edges), it is equivalent to the molecular constitution. The *molecular graph* contains more information, because it has been defined as the embedded graph of a molecule, to take into account the fact that molecules are not abstract entities but real objects in 3D space [3, 4]. The molecular graphs of topological stereoisomers (including enantiomers) cannot be converted into each other by continuous deformations, whatever their amplitude. Walba, in his seminal paper about topological stereochemistry, defined an edge of the molecular graph to be a covalent bond and chose to leave open the question of a topologically significant bond. Topological stereoisomers are operationally distinct as long as, under the conditions of observation, the bonds involved in the graph are not labile – that is, cannot be broken and reformed [3].

Classical molecules exhibiting topological steroisomerism are those having the topology of knots and links [54]. Figure 1.26 shows the diagrams of the four first prime knots, including the unknot (a). The trefoil knot (b) has three crossings, the figure-of-eight knot (c) four, the pentafoil knot (d) five, etc. The simplest link is the Hopf link (f), which is made of a pair of singly interlocked rings. The Solomon link (g) is a pair of doubly interlocked rings. Of the links made from three subunits, the "Borromean rings" have a remarkable topology because they are formed from three interlocked rings that form disjointed pairs. Links and knots that have been realized chemically are the trefoil, the pentafoil, and the figure-of-eight knot on the one hand, and the Hopf and the Solomon links, and the "Borromean rings," on the other hand.

1.3.2 Topological Chirality

A chiral molecule is topologically chiral if and only if its enantiomers cannot be converted into each other by a continuous deformation [55, 56]. Such a property can be proved only by mathematical methods. On the other hand, topological achirality of a molecule is demonstrated by finding at least one achiral presentation of its molecular graph. For example, the trefoil knot has been shown to be topologically chiral, whereas the figure-of-eight knot is topologically achiral, because it has a S_4-symmetric presentation. However, the lack of the existence of at least one achiral presentation does not imply topological chirality, as exemplified by the so-called topological "rubber gloves" [57], which are topological analogs of the biphenyls mentioned in section 1.2.2.1.

The discovery that dynamic bonds (i.e., labile bonds that can be cleaved and reformed reversibly in certain conditions) can be used for the synthesis of topologically nonplanar molecules has opened a completely new field of investigations in molecular topology

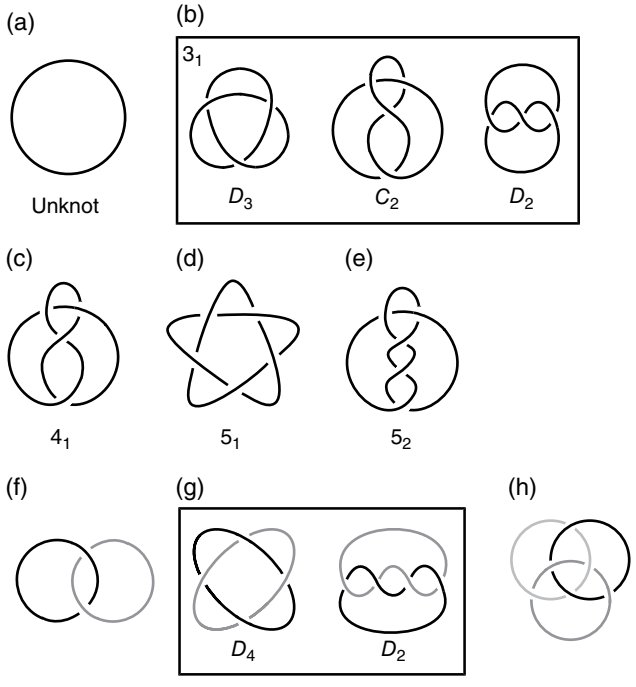

Figure 1.26 *Diagrams of the four first prime knots, (a) unknot, (b) 3_1 (trefoil knot, shown as its three common diagrams), (c) 4_1 (figure-of-eight knot; compare with the diagram of C_2 symmetry of 3_1), (d) 5_1 (pentafoil knot), (e) 5_2, (f) Hopf link, (g) Solomon link, (h) Borromean rings*

[58, 62]. Essentially, these bonds are either coordination bonds (e.g., palladium–nitrogen, gold–phosphorus), or covalent bonds (e.g., imine and disulfide being the most commonly used), and/or their combination (e.g., the formation of imine bonds under first-row transition metal templation). As the formation of these bonds operates under thermodynamic control, the reactions lead to mixtures of topological stereoisomers. *Sensu stricto*, only bonds that are not reversibly created and cleaved under the conditions of observation should be considered as topologically relevant, which limits them to classical covalent and some coordination bonds (those in the range above 30 kcal × mol^{-1}). In fact topological chirality can be considered from the formal or the operational viewpoint. Whereas the first case concerns the manipulation of graphs, the second concerns experiment. A molecule that is demonstrated to be topologically chiral based on a formal graph, may not be operationally (topologically) chiral because some of the bonds involved in the graph are reversible under the conditions of observation. Reciprocally, a molecule that is demonstrated to be chiral experimentally will obviously not be necessarily topologically chiral.

1.3.3 Topologically Relevant Molecules that are not Topologically Chiral

This section examines systems that are not topogically chiral, yet they have a nontrivial topology in relation to chirality. In fact they are topological analogues of the molecular rubber gloves discussed in section 1.2.2.1.